Am J Transl Res 2026;18(9):8481-8500
www.ajtr.org /ISSN:1943-8141/AJTR0174989

*Original Article*

# MIF promotes the progression of breast cancer by combining with CD74 to drive macrophage M2 polarization

Jinwan Li[1*], Yongjian Zhou[2*], Tengyue Yan[2], Shengkang Dai[3], Jing Leng[1,4]

*[1]Department of Immunology, School of Basic Medical Sciences, Guangxi Medical University, Nanning 530021, Guangxi, China; [2]Institute of Life Sciences, Guangxi Medical University, Nanning 530021, Guangxi, China; [3]Department of Gynecology, The Second Affiliated Hospital of Guangxi University of Chinese Medicine, No. 10 Huadong Road, Nanning 530011, Guangxi, China; [4]Guangxi Key Laboratory of Translational Medicine for Treating High Incidence Infectious Diseases with Integrative Medicine, Guangxi University of Chinese Medicine, Nanning 530200, Guangxi, China. [*]Equal contributors and co-first authors.*

Received June 26, 2026; Accepted August 27, 2026; Epub September 15, 2026; Published September 30, 2026

**Abstract:** Background: Breast cancer (BRCA) is one of the most prevalent malignancies in women. Macrophage migration inhibitory factor (MIF) and its receptor CD74 molecule (CD74) have been implicated in tumor immunity, yet their functional interplay within the BRCA microenvironment remains unclear. Methods: Transcriptomic datasets and single-cell RNA sequencing analyses were performed to assess the expression patterns, prognostic significance, and cellular localization of MIF and CD74. Their functional interactions were further investigated using an in vitro co-culture system of MCF7 BRCA cells and macrophages, combined with MIF inhibition and CD74 blockade. Results: MIF and CD74 were significantly upregulated in BRCA and associated with poor prognosis. Single-cell analysis showed that CD74 was predominantly expressed in tumor-associated macrophages, whereas MIF was mainly produced by cancer cells. Tumor-derived MIF promoted M2 macrophage polarization through CD74-mediated activation of the phosphoinositide 3-kinase (PI3K)/protein kinase B (AKT) signaling pathway, and this effect was abolished upon disruption of this signaling axis. Hypoxia was identified as a critical upstream regulator driving MIF secretion. Conclusions: These findings identify a hypoxia-driven MIF/CD74 signaling axis that promotes immunosuppressive macrophage polarization in BRCA, highlighting its potential as a therapeutic target.

**Keywords:** CD74, MIF, breast cancer, macrophage, polarization

## Introduction

Breast cancer (BRCA) is the most common malignant tumor among women worldwide [1]. Its hypoxic tumor microenvironment (TME) is closely associated with disease progression and poor prognosis. Recent studies have revealed that macrophage migration inhibitory factor (MIF), a pleiotropic inflammatory cytokine, is upregulated under hypoxic conditions and plays a role in tumor progression by modulating the immune microenvironment [2-4]. However, the molecular mechanisms through which MIF promotes immune evasion through macrophage polarization in the hypoxic BRCA microenvironment remains unclear.

MIF is an important inflammatory mediator involved in various cellular processes, especially cancer initiation and progression. Under hypoxia conditions, activation of hypoxia-inducible factor 1-alpha (HIF-1α) in BRCA cells significantly increases MIF expression [2, 5]. Culturing MCF7 cells at 1% $O_2$ for 48 hours can mimic the hypoxic tumor microenvironment, providing an appropriate model for investigating the mechanism underlying MIF induction [6, 7]. Recombinant MIF has been shown to stimulate the proliferation of BRCA cell lines [8]. MIF depletion in BRCA cells increased intratumoral cytolytic $CD8^+$ T cell infiltration and enhanced pro-inflammatory macrophage responses, suggesting that MIF may represent an attractive therapeutic target to circumvent metabolic reprogramming and immunosuppression in BRCA [9].

MIF exerts its biological functions primarily through binding to its receptor, CD74 molecule (CD74). Lue et al. reported that MIF interacted

https://doi.org/10.62347/DYIB6926

with its receptor CD74 to promote cell survival by activating the phosphoinositide 3-kinase (PI3K)/protein kinase B (AKT) signaling pathway [10]. Wirtz et al. demonstrated that MIF-CD74 interaction significantly promoted tumor progression in a hepatocellular carcinoma model [11]. Notably, the effects of MIF on macrophage polarization appears to be highly context-dependent. For instance, in a non-tumor inflammatory model, Yang et al. demonstrated that MIF deficiency reduced macrophage recruitment, promoted the transition from M1 to M2 polarization, and enhanced regulatory T-cell (Treg) responses [12]. In contrast, within the TME, where MIF is frequently overexpressed by malignant cells, emerging evidence indicates that MIF acts as a pro-tumorigenic factor by promoting macrophage polarization toward an M2-like phenotype. Specifically, in a non-small cell lung cancer brain metastasis model, radiotherapy promoted microglia M1 polarization and increased radiosensitivity by blocking the MIF-CD74 axis and reducing HIF-1α-dependent MIF secretion [13]. However, whether tumor-derived MIF directly drives M2 polarization in BRCA through the CD74/PI3K/Akt axis remains largely unexplored. To address this knowledge gap, we established a co-culture system using THP-1-derived macrophages and MCF7 conditioned medium (CM), combined with interventions using the MIF inhibitor ISO-1 and the CD74-blocking antibody Milatuzumab, to further elucidate the role of this pathway in the BRCA immune microenvironment.

Recent studies have highlighted the critical role of TME in BRCA aggressiveness and treatment failure. The TME consists of multiple components, including immune cells, fibroblasts, and extracellular matrix proteins [14]. Tumor-associated macrophages (TAMs) play a critical role in BRCA progression. Increased TAMs density has been correlated with poor prognosis in BRCA [15]. Depletion of macrophages from tumor sites delayed tumor progression in mouse models of BRCA [15]. Furthermore, elevated macrophage infiltration was significantly associated with both shorter relapse-free survival and worse overall survival, establishing macrophage infiltration as an independent prognostic factor [16]. TAMs acquire an M2-like phenotype driven by tumor-derived and T cell-derived cytokines [17]. The predominance of M2-like TAMs in BRCA contributes to an immunosuppressive phenotype [18-20]. These findings indicate that M2 macrophages play a critical role in BRCA progression. Therefore, elucidating the molecular mechanisms underlying macrophage M2 polarization in BRCA tissues is of substantial importance.

In this study, we investigated MIF/CD74 expression patterns and their prognostic value in BRCA, and further explored the mechanism by which MIF stimulates macrophage M2 polarization through CD74 engagement. These findings provided new insights into targeting the MIF-CD74 interaction as a potential therapeutic strategy for BRCA.

## Methods

### *Cell lines and cell culture*

The MCF7 (SCSP-531) and THP-1 (SCSP-567) cell lines were purchased from the National Collection of Authenticated Cell Cultures. Both cell lines tested negative for mycoplasma contamination and were authenticated by short tandem repeat profiling. MCF7 cells were cultured in MEM (Gibco, 11095080, Thermo Fisher Scientific, Inc.) supplemented with 10% FBS (Gibco, 10099141C, Thermo Fisher Scientific, Inc.), 1% NEAA (Gibco, 11140050, Thermo Fisher Scientific, Inc.), and 0.01 mg/mL human recombinant insulin (SIGMA, 91077C-1G). THP-1 cells were cultured in RPMI 1640 medium (Gibco, 11875093, Thermo Fisher Scientific, Inc.) supplemented with 10% FBS (Gibco, 10099141C, Thermo Fisher Scientific, Inc.) and 0.05 mM BME (Gibco, 21985023, Thermo Fisher Scientific, Inc.). All cells were cultured in a cell culture incubator containing 5% $CO_2$ at 37°C.

To investigate hypoxia-induced MIF production in BRCA cells, MCF7 cells were incubated under hypoxic conditions (1% $O_2$) for 48 hours. To evaluate the role of HIF-1α in MIF regulation, MCF7 cells were co-cultured with 50 μM PX-478 (an inhibitor of HIF-1α; MedChemExpress, HY-10231) for 48 h.

The effect of MCF7-derived MIF on macrophage polarization was evaluated by incubating THP-1-derived macrophages with conditioned medium (CM) collected from MCF7 cells for 48 hours. Specific interventions were applied as follows: (1) To inhibit MIF, ISO-1 (MedChemExpress, HY-16692) was added to MCF7-derived CM at a final concentration of 20 μM.

(2) To block CD74 signaling, THP-1 cells were pre-incubated with 5 μg/mL anti-CD74 antibody Milatuzumab (MedChemExpress, HY-P99731). DMSO was added to the RPMI 1640 medium as the vehicle control.

To further confirm that hypoxia-induced MIF promotes macrophage M2 polarization through the PI3K-AKT signaling pathway, rescue experiments were performed using the PI3K inhibitor LY294002 (MedChemExpress, HY-10108) at 30 μM for 48 h.

*siRNA transfection*

MIF siRNA transfection was performed using RNA TransMate according to the manufacturer's protocol. Mixture of siRNA and RNA TransMate was prepared in serum-free RPMI 1640 medium and subsequently added to the cell culture medium.

*Data collection and analysis*

The Gene Expression Omnibus (GEO) database (http://www.ncbi.nlm.nih.gov/geo) was used to obtain transcriptomic datasets. The GSE45419 datasets, including 24 breast tumor tissues and 8 benign breast lesions, and the GSE229571 dataset, including 6 breast tumor tissues and 6 normal tissues, were downloaded for analysis. Data analysis was performed using R software (version 4.2.0). Differentially expressed genes (DEGs) (*P*-value < 0.05, |log2 fold-change (logFC)| > 1) were identified using the limma package.

The Human Protein Atlas (HPA) portal provides an open-access platform integrating proteomics, transcriptomics, and systems biology data, enabling the exploration of protein expression profiles across diverse tissues and organs. The database includes information regarding subcellular localization and expression patterns in both tumor and normal tissues [21]. In this study, we particularly focused on CD74 expression patterns in both normal and tumor tissues. The expression levels and distribution characteristics of CD74 were investigated to provide insights into its potential role in BRCA development and progression.

*scRNA-seq analysis*

The scRNA-seq GSE268662 dataset (5 breast tumor tissues and 4 normal tissues) was downloaded from the GEO database. Downstream analyses were conducted using the Seurat toolkit (version 4.1.1) in the R statistical environment (version 4.2.0). Principal component analysis (PCA) was performed using RunPCA function for dimensionality reduction, and the top 30 principal components were retained for subsequent analyses. Batch effect correction was applied across all samples using RunHarmony from the Harmony package (version 0.1.0). A shared nearest-neighbor (SNN) graph was constructed using the FindNeighbors function based on the top 30 principal components. Cell clustering was performed using the FindClusters function with a resolution parameter of 0.7. Nonlinear dimensionality reduction for visualization was achieved using RunUMAP. Cluster-specific genes were identified using FindAllMarkers function based on the Wilcoxon rank-sum test. Genes with avg_log2FC > 0.25 and *P*_val_adj < 0.05 were considered significant marker genes. Cell types were annotated according to established canonical markers. The expression pattern of CD74 across annotated cell clusters was visualized using the FeaturePlot function, while CD74 expression levels across individual cell populations were further evaluated using DotPlot and ViolinPlot functions.

*Prognostic analysis*

To evaluate the prognostic significance of CD74 in patients with BRCA, the Gene Expression Profiling Interactive Analysis (GEPIA) platform was utilized. GEPIA is a gene expression analysis platform based on data from The Cancer Genome Atlas and The Genotype-Tissue Expression databases, incorporating extensive transcriptomic information from both tumor and normal tissues [22]. Due to its efficiency and accessibility, GEPIA has been widely applied in cancer-related studies. In this study, GEPIA was used to analyze CD74 expression patterns and their relationship with clinical prognosis in patients with BRCA, providing a basis for subsequent investigations.

*RT-qPCR*

Primers were designed and synthesized by Sangon Biotech (Shanghai, China). Total RNA was extracted from cells using the RNAEx ZOL RNA Extraction Kit (ECOTOP, China). RNA was reverse-transcribed into complementary DNA

(cDNA) using the Hifair III First Strand cDNA Synthesis Kit (YEASEN, China). The mRNA expression level was then detected using HiEff qPCR SYBR Green Master Mix (YEASEN, China) and determined via the $2^{\Delta\Delta Ct}$ method. The primer sequences are shown as follows: MIF, F: ATGTGGGCTGGAACAACTCC, R: TTTCTCCCCACCAGAAGGTTG; mannose receptor C-type 1 (MRC1, CD206), F: TACCTGCGACAGTAAACGAG, R: CCTGGCTATAAGGGAATTGTG; CD163 molecule (CD163), F: GCACGAGGACAGTGTTTGG, R: GCGACCTCCTCCATTTACC; arginase 1 (ARG1), F: CAGACTAGGAATTGGCAAGG, R: GGGTCCAGTCCGTCAACATC; actin beta (ACTB), F: GTGACAGCAGTCGGTTGGAG, R: GTGGGGTGGCTTTTAGGATG.

*Transcriptome analysis*

Transcriptome sequencing was performed to investigate gene expression changes in MCF7 cells cultured under normoxic and hypoxic conditions. RNA sequencing was performed by Wuhan Benagen Technology Co., Ltd. (Wuhan, China). Library construction was performed using the VAHTS Universal V6 RNA-seq Library Prep Kit (Vazyme, China). Briefly, mRNA was enriched using magnetic beads and fragmented into 200-300 bp segments. First-strand cDNA was synthesized using random hexamer primers and M-MuLV reverse transcriptase. Then, second-strand cDNA synthesis was performed using DNA polymerase I and RNase H with dUTP incorporation for strand-specific labeling. The resulting cDNA fragments were end-repaired, with A-tailed, and ligated with sequencing adapters. Library amplification was performed using high-fidelity DNA polymerase with universal and index primers, followed by purification using AMPure XP beads. Library quality was assessed using Qubit 3.0. Library integrity was assessed using the Agilent 2100 Bioanalyzer. Next, the concentration was quantified by qPCR. Finally, sequencing was performed on the DNBSEQ-T7 platform using a PE150 sequencing strategy.

*Western blot*

Protein expression levels were determined by Western blot. Total protein was extracted from RIPA lysate (Solarbio, R0010) with protease and phosphatase inhibitor (Abcam, ab201119). Then supernatant was extracted after centrifugation and protein content was determined using a BCA kit (Solarbio, PC0020). The protein samples were mixed with 5× sample loading buffer (Solarbio, P1040) and heated at 100°C for 10 min. A volume of 40 μg total protein was added to each lane. The total protein was separated by SDS-PAGE and then electrotransferred onto a PVDF membrane (Millipore, ISEQ00010). The PVDF membrane was incubated with a 5% skim milk (OXOID, LP0033B) solution for 1.5 h at room temperature. The primary antibody was incubated after dilution overnight at 4°C. The secondary antibody was incubated after dilution for 1 h at room temperature. The PVDF membrane was visualized with an enhanced chemiluminescence detector system (Tanon). The antibodies used were as follows: HIF-1α (Abcam, ab179483), PI3K (Proteintech, 60225-1-Ig), p-PI3K (Proteintech, 82796-4-RR), AKT (Abcam, ab179463), p-AKT (Abcam, ab183758), MIF (Abcam, ab176565), glyceraldehyde-3-phosphate dehydrogenase (GAPDH) (Abcam, ab181602), Goat Anti-Rabbit IgG (Abcam, ab6721), Goat Anti-Mouse IgG (Abcam, ab6789).

*ELISA analysis*

MIF secretion levels in the CM collected from MCF7 cells, as well as interleukin 10 (IL-10) and transforming growth factor beta 1 (TGF-β1) secretion levels in the CM from macrophages were quantified using human ELISA Kit (MIF, MULTISCIENCES, EK1158; IL-10, MULTISCIENCES, EK110; TGF-β1, MULTISCIENCES, EK981) according to the manufacturer's protocol. Briefly, standards, test samples, and biotinylated detection antibodies were added to the microplate wells and incubated for 2 hours. After washing, streptavidin-HRP was added and incubated. Subsequently, TMB substrate was added, and the plates were incubated in the dark. The reaction was terminated by adding stop solution, and absorbance was measured at 450 nm using a microplate reader.

*Flow cytometry analysis*

Cells were washed twice with PBS and detached using Accutase at 37°C. The collected cells were centrifuged were washed with precooled PBS. Following this, cells were resuspended in PBS and incubated with 20 μL of FITC-conjugated mouse anti-human CD206 (BD Pharmingen, USA) at room temperature in the dark for 30 minutes. After staining, samples

were gently mixed and analyzed using a CytoFLEX flow cytometer (Beckman Coulter). Flow cytometry data were analyzed using FlowJo software.

*Statistical analysis*

Data are presented as the mean ± standard deviation (SD). Statistical analyses were performed using R 4.2.0 and SPSS 25.0. Comparisons between two groups were performed using independent-samples t-tests, whereas comparisons among multiple groups using one-way ANOVA. The significance levels were indicated as follows: $^{*}P < 0.05$; $^{**}P < 0.01$; and $^{***}P < 0.001$.

## Results

*CD74 was consistently upregulated in BRCA*

The GSE45419 dataset was analyzed to identify DEGs, which were visualized using a volcano plot (**Figure 1A**). To further characterize the expression pattern of CD74 in BRCA, transcriptomic analyses were performed across four datasets representing overall BRCA, estrogen receptor-positive ($ER^+$) breast cancer, human epidermal growth factor receptor 2-positive ($HER2^+$) breast cancer, and triple-negative breast cancer (TNBC). Compared with normal breast tissues, CD74 expression was significantly increased in BRCA tissues ($P < 0.05$), and this upregulation was consistently observed across all molecular subtypes analyzed (**Figure 1B-E**).

Survival analysis based on the GEPIA database showed that CD74 expression was significantly associated with patient prognosis ($P < 0.05$; **Figure 1F**). Single-cell RNA sequencing analysis identified 11 major cell types, including B cells, $CD4^+$ T cells, $CD8^+$ T cells, macrophages, endothelial cells, epithelial cells, fibroblasts, mast cells, $MKI67^+$ cells, pericytes, and plasma cells (**Figure 1G**). CD74 expression was detected across multiple cell populations in both normal and tumor tissues; however, its predominant cellular distribution differed between conditions. In normal tissues, CD74 expression was primarily enriched in B cells, whereas in tumor tissues, CD74 expression was primarily concentrated in macrophages (**Figure 1H**, **1I**).

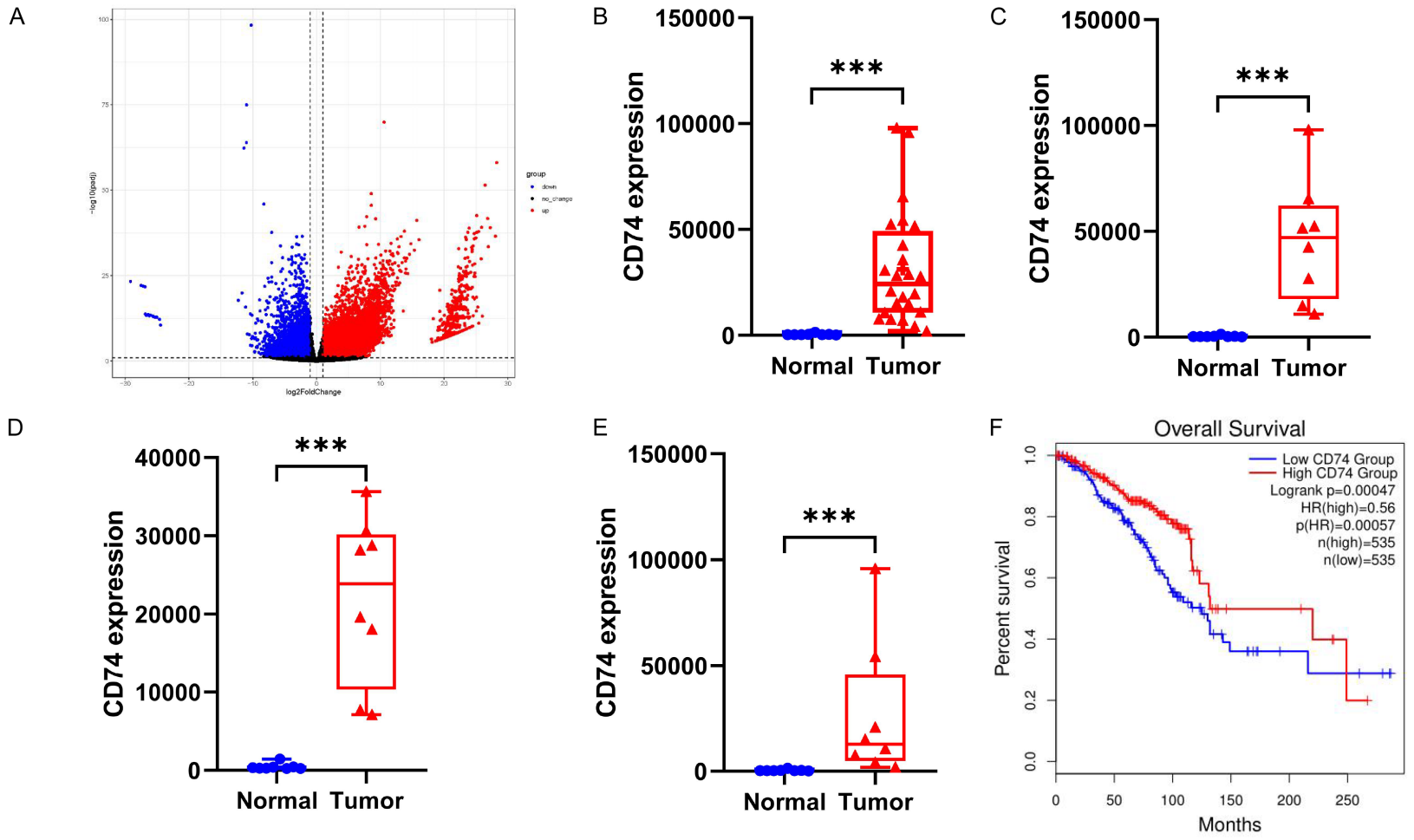
Quantitative analysis revealed significant differences in CD74 expression between tumor and normal tissues across multiple cell types, including $CD4^+$ T cells, $CD8^+$ T cells, endothelial cells, fibroblasts, macrophages, mast cells, pericytes, and plasma cells ($P < 0.05$). Notably, CD74 expression was significantly higher in macrophages derived from BRCA tissues than in those from normal breast tissues. In contrast, no statistically significant differences were observed in B cells, epithelial cells, or $MKI67^+$ cells (**Figure 1J**). These findings indicate that CD74 is preferentially upregulated in tumor-associated macrophages within the BRCA microenvironment.

*CD74 protein expression in normal breast and BRCA tissues*

Immunohistochemical data from the Human Protein Atlas (HPA) showed that CD74 staining was undetectable in adipocytes and myoepithelial cells, whereas strong staining was observed in glandular cells of normal breast tissues. In BRCA tumor tissues, CD74 displayed clearly positive staining (**Figure 2A**). In addition, immunohistochemical analysis of 12 BRCA tissue samples revealed heterogeneous CD74 expression levels, with one case exhibiting low expression, ten cases showing moderate expression, and one case showing high expression (**Figure 2B**).

*MIF expression was upregulated in BRCA tissues*

The GSE229571 dataset was analyzed to identify DEGs, and the results were visualized in a volcano plot (**Figure 3A**). Compared with normal breast tissues, MIF expression was significantly increased in BRCA tissues ($P < 0.05$; **Figure 3B**). Single-cell sequencing analysis demonstrated that MIF expression was mainly localized to epithelial cells in both normal and tumor tissues (**Figure 3C**, **3D**). Quantitative comparison further revealed significant differences in MIF expression between tumor and normal tissues across multiple cell types, including $CD4^+$ T cells, endothelial cells, epithelial cells, fibroblasts, and macrophages. Notably, MIF expression was significantly higher in epithelial cells from BRCA tissues than in epithelial cells from normal tissues ($P < 0.05$; **Figure 3E**).


A
B
C
D
E
F
group
down
no_change
up
log2FoldChange
CD74 expression
Normal
Tumor
***
Overall Survival
Low CD74 Group
High CD74 Group
Logrank p=0.00047
HR(high)=0.56
p(HR)=0.00057
n(high)=535
n(low)=535
Percent survival
Months

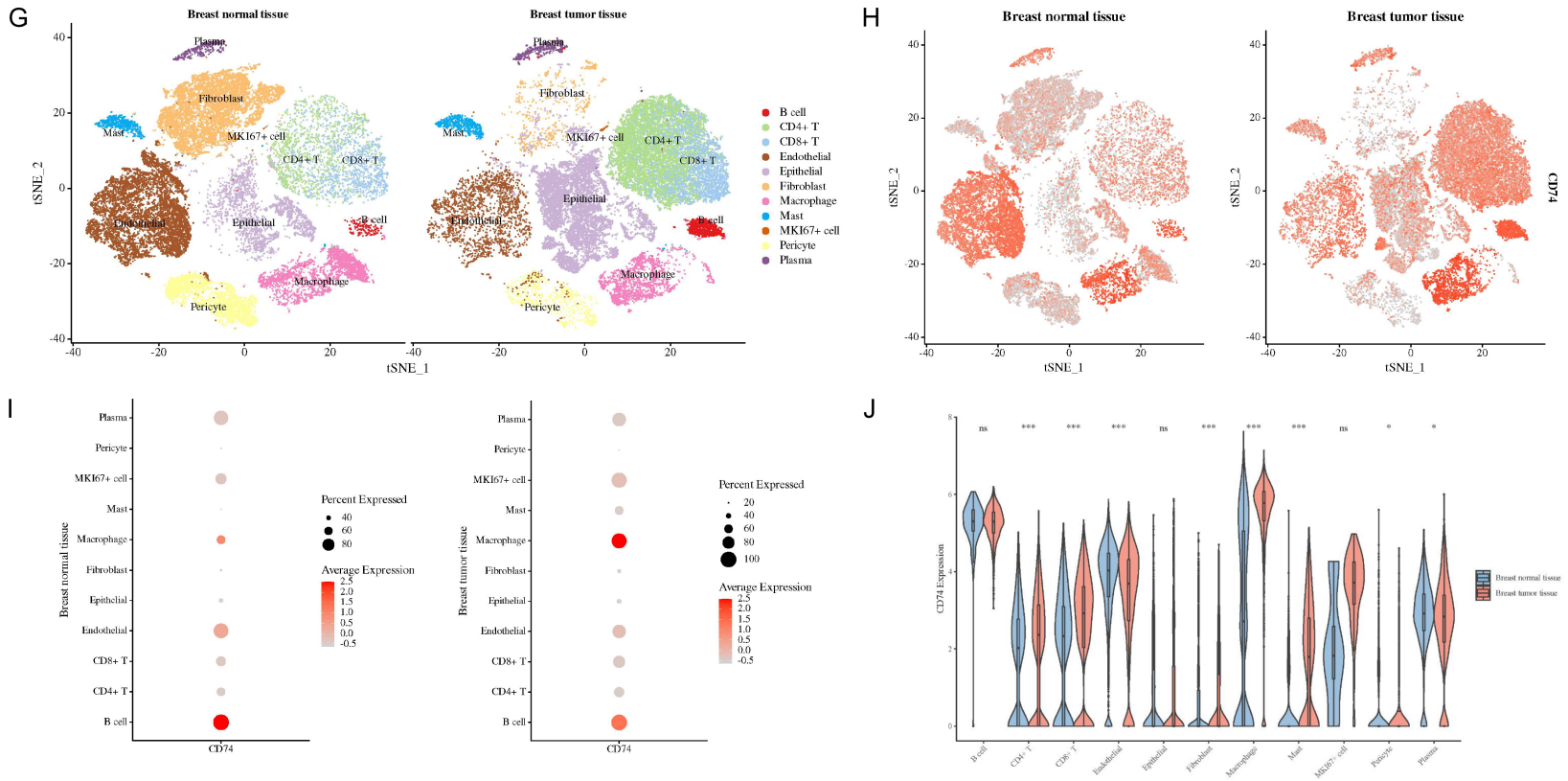



**Figure 1.** The expression of CD74 in normal and BRCA tumor tissues. A. DEGs between normal and tumor tissues were visualized through a volcano plot. B. The expression of CD74 in normal and tumor tissues. C. The expression of CD74 in normal and $ER^+$ tumor tissues. D. The expression of CD74 in normal and $HER2^+$ tumor tissues. E. The expression of CD74 in normal and TNBC tumor tissues. F. The relationship between CD74 expression and patient survival. G. UMAP plot showing annotated cell types in tumor and normal tissues. H. Differential expression of CD74 between normal and tumor tissues across cell types. I. The expression of CD74 in normal and tumor tissues. J. Statistical comparison of CD74 expression between tumor and normal tissues. Notes: DEG, differentially expressed gene; UMAP, Uniform Manifold Approximation and Projection; ns, not significant; ***, $P < 0.001$.

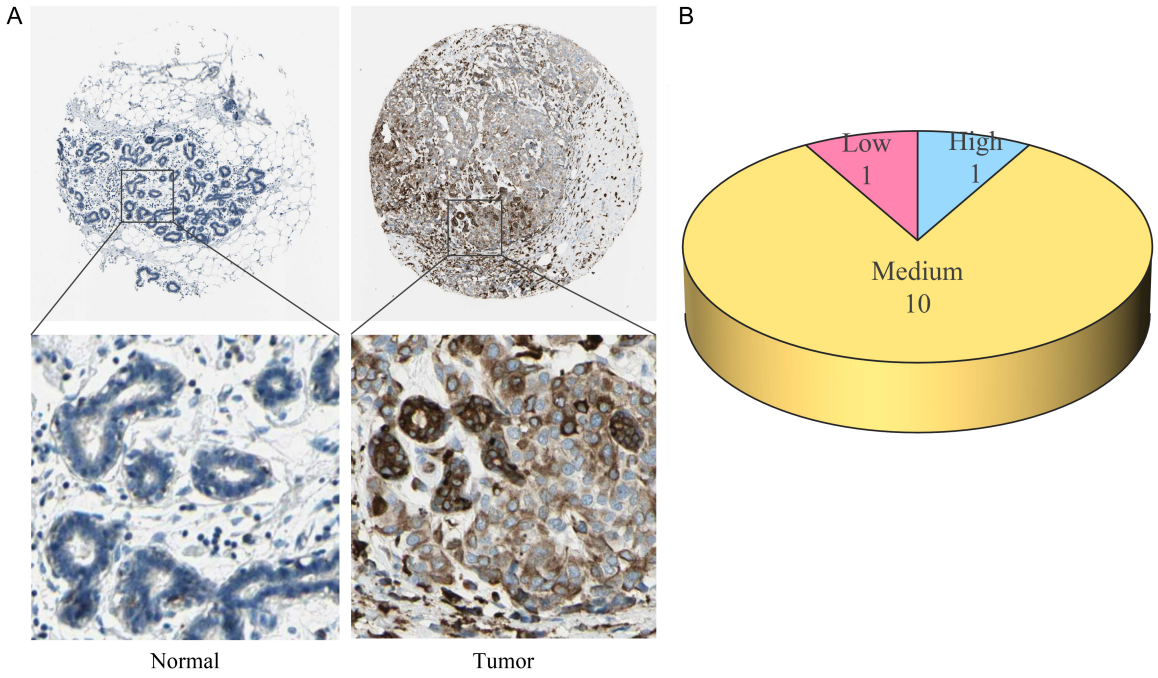



**Figure 2.** Expression profiles of CD74 in normal breast tissues and BRCA tumor tissues based on the HPA database. A. Immunohistochemical staining of CD74 in normal breast tissues and BRCA tumor tissues from the HPA database. B. Immunohistochemical staining pattern of CD74 in 12 BRCA tumor tissues from the HPA database. Notes: BRCA, breast cancer; HPA, Human Protein Atlas.

*MIF protein expression in normal breast and BRCA tissues*

Immunohistochemical staining data from the HPA database showed that MIF staining was undetectable in adipocytes, weakly expressed in myoepithelial cells, and strongly expressed in glandular cells of normal breast tissues. In BRCA tumor tissues, MIF exhibited clear positive staining (**Figure 4A**). Immunohistochemical staining of 12 BRCA tissue samples revealed heterogeneous MIF expression, with one case showing undetectable expression, two cases showing low expression, and nine cases showing moderate expression (**Figure 4B**).

*Cell-cell communication analysis identified MIF signaling between epithelial cells and macrophages*

Based on the scRNA-seq cell-type annotations, intercellular communication within tumor tissues was inferred using CellChat. Heatmaps depicting interaction numbers and interaction strengths showed strong communication between epithelial cells and macrophages (**Figure 5A**, **5B**). Directionality analysis indicated that outgoing MIF signaling was predominantly derived from epithelial cells, whereas ingoing MIF signaling was mainly enriched in $CD4^+$ T cells, $CD8^+$ T cells, and macrophages (**Figure 5C**). Consistently, the MIF signaling network showed that MIF was primarily produced by epithelial cells and interacted with receptors expressed on $CD4^+$ T cells, $CD8^+$ T cells, and macrophages (**Figure 5D**, **5E**). Ligand-receptor analysis further identified MIF-(CD74+CXCR4) and MIF-(CD74+CD44) as the most frequent interaction pairs in BRCA tissues (**Figure 5F**). Protein-protein interaction analysis from the STRING database supported an interaction between MIF and CD74 (**Figure 5G**, **5H**).

*Hypoxia promoted MIF expression in BRCA cells through HIF-1α*

To explore the mechanism underlying increased MIF expression, transcriptomic data from MCF7 cells cultured under normoxic and hypoxic conditions were analyzed. The results showed that hypoxia significantly increased MIF expression (**Figure 6A**, **6B**). This finding was further supported by increased MIF mRNA levels detected by PCR and elevated MIF protein levels mea-

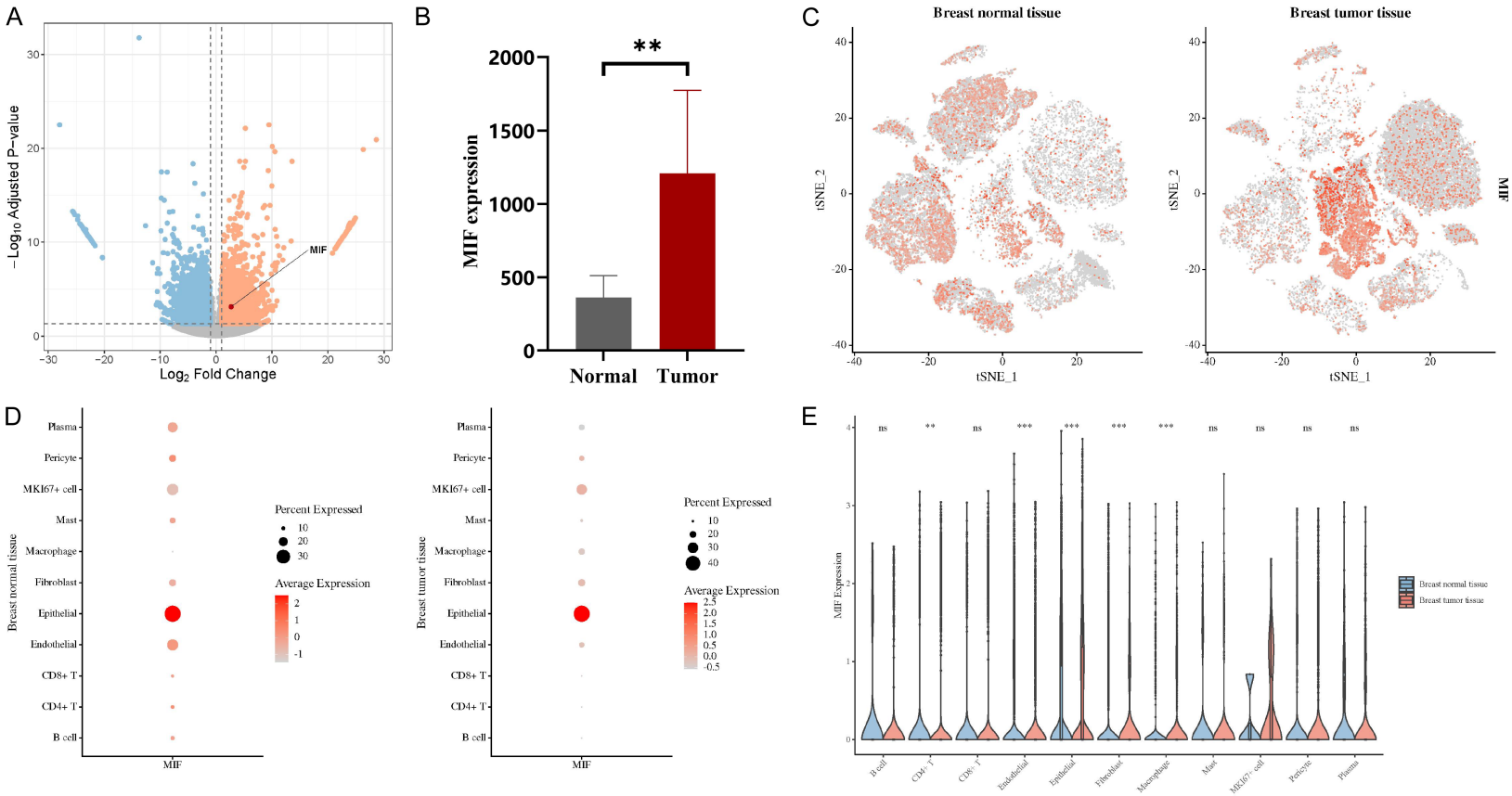



**Figure 3.** The expression of MIF in normal and BRCA tumor tissues. A. DEGs between normal and tumor tissues were visualized through a volcano plot. B. The expression of MIF in normal and tumor tissues. C. Differential expression of MIF between normal and tumor tissues across cell types. D. The expression of MIF in normal and tumor tissues. E. Statistical comparison of MIF expression between tumor and normal tissues. Notes: MIF, macrophage migration inhibitory factor; DEG, differentially expressed gene; ns, not significant; **, $P < 0.01$; ***, $P < 0.001$.

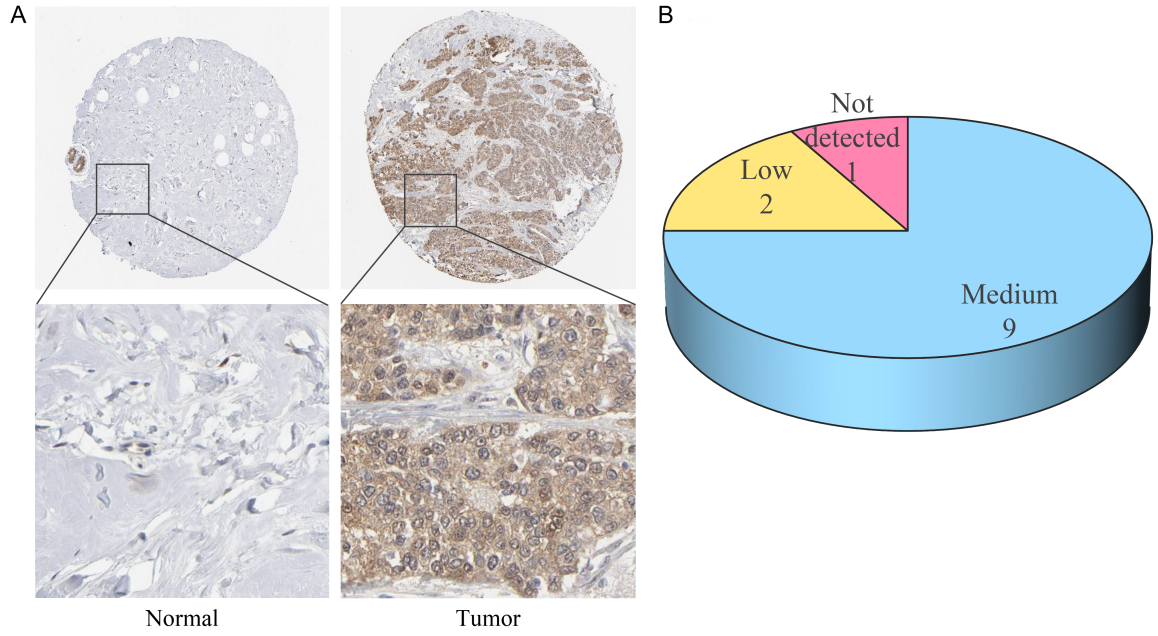



**Figure 4.** Expression profiles of MIF in normal breast tissues and BRCA tumor tissues based on the HPA database. A. Immunohistochemical staining of MIF in normal breast tissues and BRCA tumor tissues from the HPA database. B. Immunohistochemical staining pattern of MIF in 12 BRCA tumor tissues from the HPA database. Notes: MIF, macrophage migration inhibitory factor; HPA, Human Protein Atlas.

sured by ELISA (**Figure 6C**, **6D**). Furthermore, Western blot analysis demonstrated that protein expression levels of HIF-1α and MIF were increased under hypoxic conditions compared with normoxic conditions (**Figure 6E**). The protein expression of HIF-1α was downregulated after incubation with 50 μM PX-478 (an inhibitor of HIF-1α) for 48 h (**Figure 6F**). In addition, both mRNA and protein expression of MIF were decreased after incubation with PX-478 (**Figure 6F-H**). These findings indicate that hypoxia induces MIF expression in BRCA cells in a HIF-1α-dependent manner.

*Tumor cell-derived and hypoxia-induced MIF mediated macrophage M2 polarization*

To investigate the role of MIF in macrophage M2 polarization, MCF7 cells were subjected to MIF knockdown using siRNA. After siRNA interference, the mRNA and protein expression of MIF significantly decreased (**Figure 7A-C**). After incubation of macrophages with CM from MCF7 cells, CM derived from siMIF-treated cells significantly decreased the mRNA expression of M2 polarization markers, including CD206, CD163, and ARG1 (**Figure 7D-F**). Flow cytometry analysis demonstrated that CD206 protein expression was also significantly decreased (**Figure 7G**, **7H**). In addition, siMIF-derived CM reduced the secretion levels of IL-10 and TGF-β1 from M2 macrophages (**Figure 7I**, **7J**).

*MIF promoted macrophage M2 polarization through CD74*

To investigate the effect of tumor-derived MIF on macrophage polarization, macrophages were exposed to CM from MCF7 cells. Compared with the control group, MCF7-derived CM significantly increased the expression of M2-like macrophages markers, including CD206, CD163 and ARG1. This effect was markedly attenuated following MIF inhibition with ISO-1 or CD74 blockade with Milatuzumab, suggesting that MIF promotes macrophage M2 polarization through CD74 signaling (**Figure 8A-C**). Flow cytometric detection of CD206 also showed similar results (**Figure 8D**, **8E**). The protein expression levels of PI3K, p-PI3K, AKT and p-AKT were detected to investigate the downstream signaling pathways involved in MIF-CD74-mediated macrophage polarization. MCF7-derived CM increased the phosphorylation levels of PI3K and AKT compared with the control group, whereas this effect was reduced

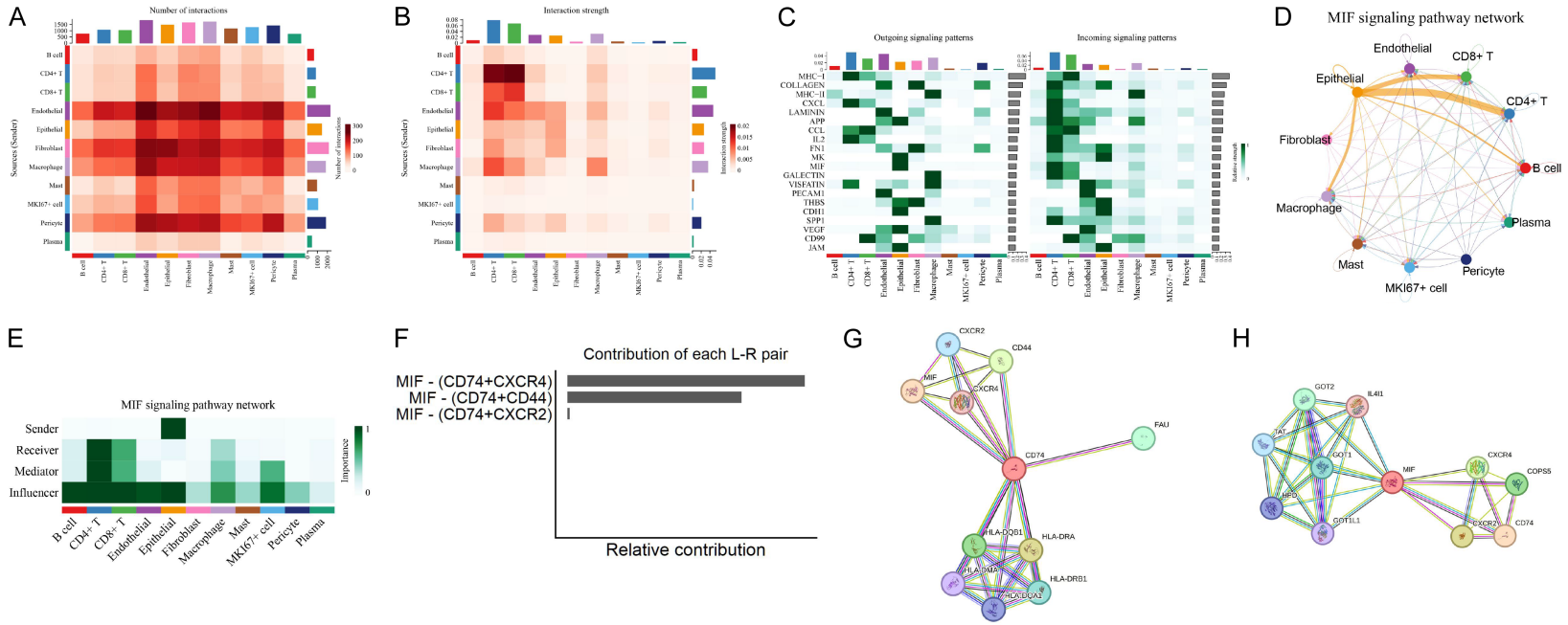



**Figure 5.** Cell-cell communication and protein-protein interaction in tumor tissue. A. Heatmaps showing the interaction numbers of cell-cell communication. B. Heatmaps showing interaction weights of cell-cell communication. C. Signaling patterns between cells. D. Network graph of intercellular interactions in the MIF signaling pathway. E. Heatmap of network centrality metrics in the MIF signaling pathway. F. MIF - (CD74 + CXCR4) and MIF - (CD74 + CD44) were the most common crosstalk in BRCA. G. Proteins that interact with CD74. H. Proteins that interact with MIF. Note: MIF, macrophage migration inhibitory factor.

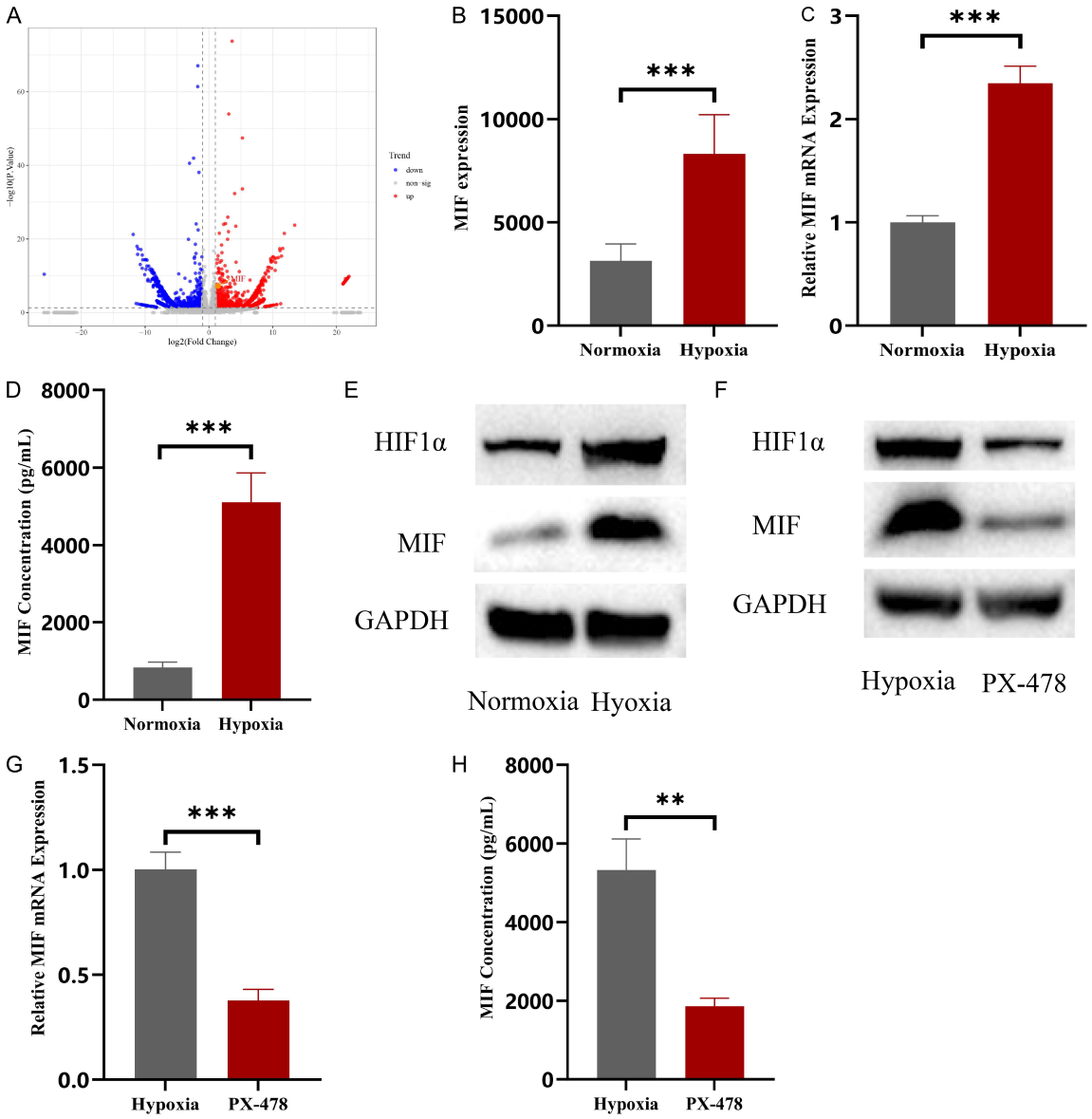



**Figure 6.** Hypoxia promoted MIF expression through the HIF1α pathway. A. Heatmap showing the DEGs between MCF7 cells cultured under normoxic and hypoxic conditions. B. Hypoxia promoted MIF production. C. PCR results indicated that hypoxia promoted MIF mRNA levels. D. ELISA results indicated that hypoxia promotes MIF protein levels. E. Hypoxia promoted the expression of HIF1α and MIF. F. PX-478 inhibited the expression of HIF1α and MIF. G. PX-478 inhibited the mRNA expression of MIF. H. PX-478 inhibited the protein expression of MIF. Notes: MIF, macrophage migration inhibitory factor; DEG, differentially expressed gene; **, $P < 0.01$; ***, $P < 0.001$.

following treatment with ISO-1 (a MIF inhibitor) or Milatuzumab (an anti-CD74 monoclonal antibody) (**Figure 8F**). In addition, MCF7-derived CM enhanced the secretion of IL-10 and TGF-β1 from M2 macrophages, and this effect was attenuated by MIF inhibition or CD74 blockade (**Figure 8G**, **8H**).

Macrophages cultured with CM derived from hypoxia- conditioned MCF7 cells exhibited more pronounced increases in CD206, CD163, and ARG1 expression compared with those cultured with CM from normoxic MCF7 cells (**Figure 9A-C**). Flow cytometric analysis of CD206 also showed similar results (**Figure 9D**, **9E**). Hypoxic CM also increased p-PI3K and p-AKT expression in macrophages compared with normoxic CM (**Figure 9F**). Furthermore, CM from hypoxia-treated MCF7 cells enhanced IL-10 and TGF-β1 secretion by M2 macro-

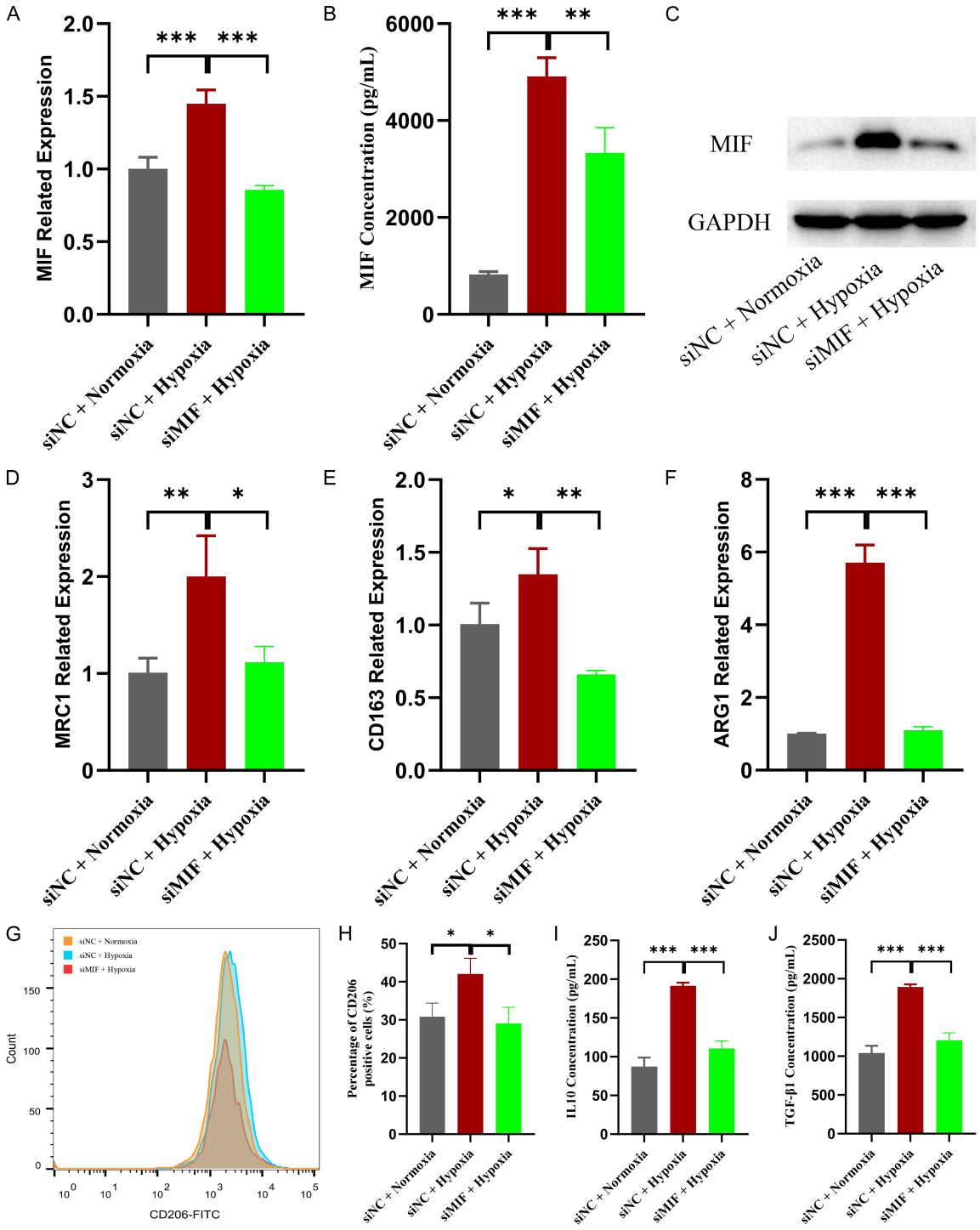



**Figure 7.** Tumor cell-derived MIF mediated hypoxia-induced macrophage M2 polarization. A. The mRNA expression of MIF. B. MIF concentration in MCF7 cell culture medium. C. The protein expression of MIF. D. The mRNA expression of MRC1 (CD206). E. The mRNA expression of CD163. F. The mRNA expression of ARG1. G. Flow cytometry results of CD206 on macrophages. H. Percentage of CD206-positive macrophages. I. Concentration of IL-10 in macrophage culture medium under different co-culture conditions. J. Concentration of TGF-β1 in macrophage culture medium under different co-culture conditions. Notes: MIF, macrophage migration inhibitory factor; *, $P < 0.05$; **, $P < 0.01$; ***, $P < 0.001$.

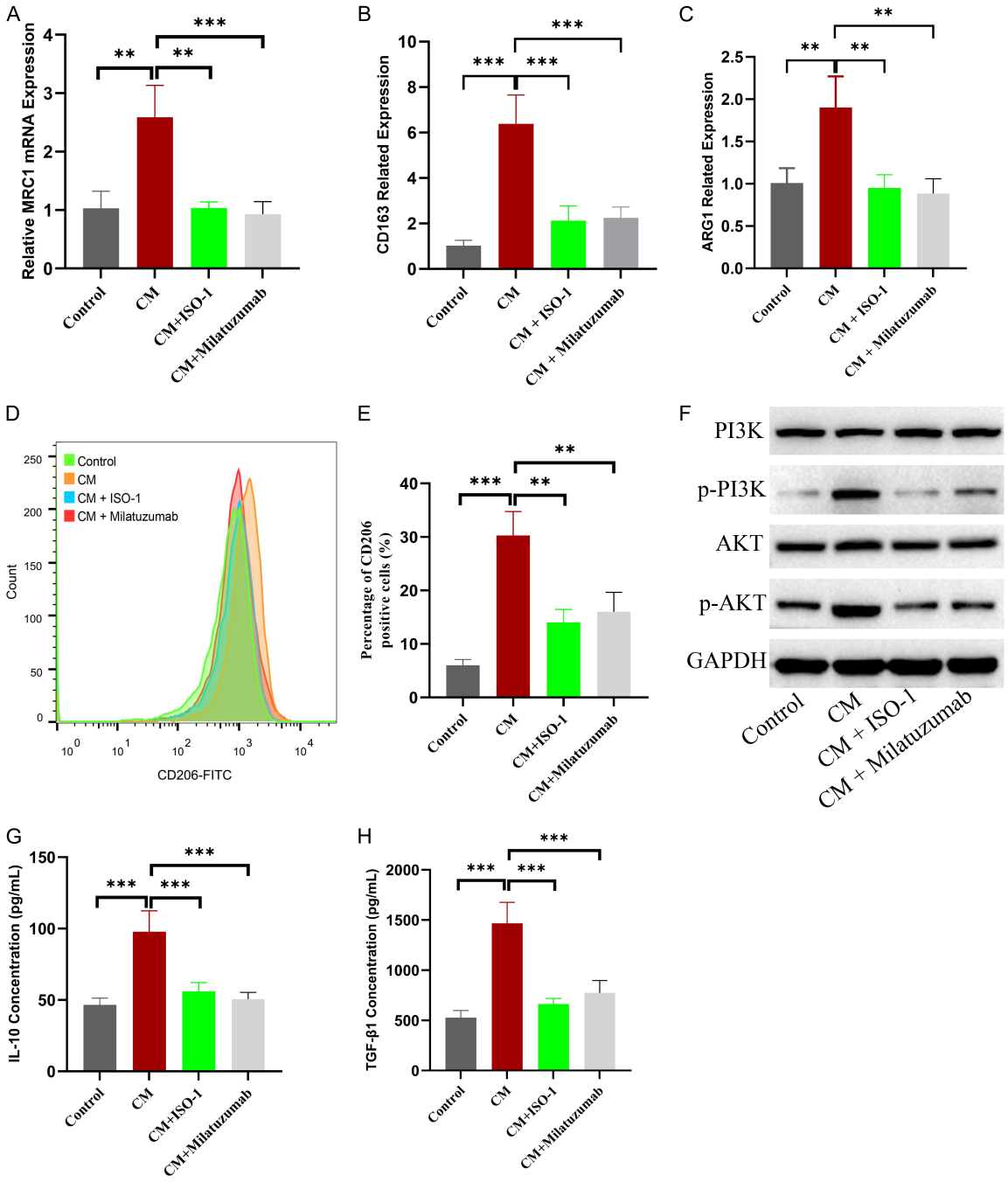



**Figure 8.** MIF promoted macrophage M2 polarization through CD74. A. The mRNA expression of MRC1 (CD206). B. The mRNA expression of CD163. C. The mRNA expression of ARG1. D. Flow cytometry analysis of CD206 on macrophages. E. Percentage of CD206-positive macrophages. F. The protein expression of PI3K-AKT signaling pathway. G. Concentration of IL-10 in macrophage culture medium under different co-culture conditions. H. Concentration of TGF-β1 in macrophage culture medium under different co-culture conditions. Notes: **, $P < 0.01$; ***, $P < 0.001$.

phages (**Figure 9G**, **9H**). Collectively, these results indicate that hypoxia-enhanced MIF secretion from MCF7 cells promotes macrophage M2 polarization through CD74 -associated signaling.

*PI3K/AKT signaling is required for MIF/CD74-mediated macrophage M2 polarization*

To further determine whether hypoxia-induced MIF promotes macrophage M2 polarization

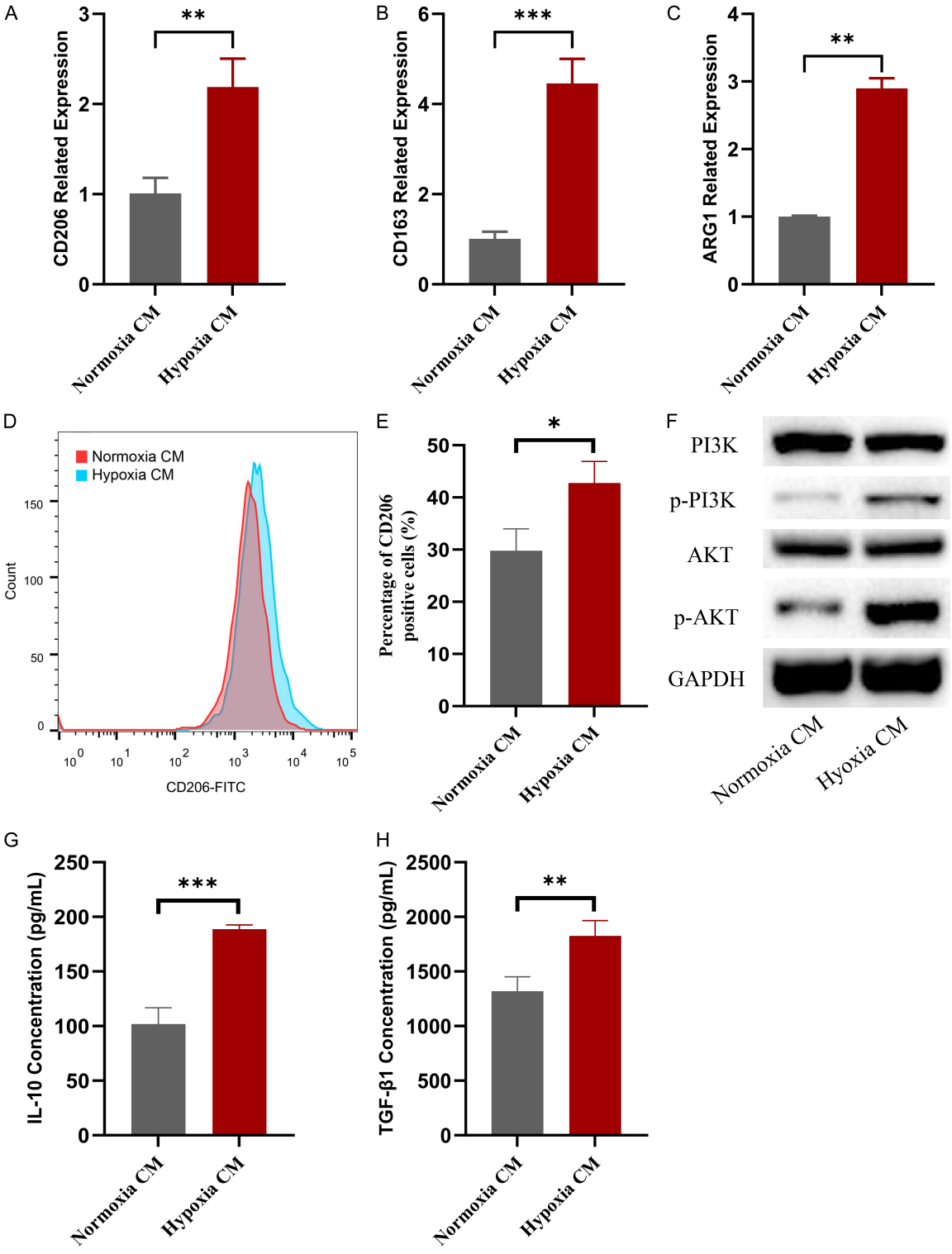



**Figure 9.** Hypoxic CM promoted M2 polarization. A. The mRNA expression of MRC1 (CD206) of macrophages. B. The mRNA expression of CD163 of macrophages. C. The mRNA expression of ARG1 of macrophages. D. Flow cytometry results of CD206 on macrophages. E. Percentage of CD206-positive macrophages. F. Western blot analysis of PI3K/AKT signaling pathway activation in macrophages under different co-culture conditions. G. Concentration of IL-10 in macrophage culture medium under different co-culture conditions. H. Concentration of TGF-β1 in macrophage culture medium under different co-culture conditions. Notes: *, $P < 0.05$; **, $P < 0.01$; ***, $P < 0.001$.

through the PI3K-AKT signaling pathway, rescue experiments were performed using LY294002 (a PI3K inhibitor). Compared with the control group, hypoxia-conditioned MCF7-derived CM significantly increased the expression levels of the M2 macrophages markers, including CD206, CD163, and ARG1. These effects were attenuated by CD74 blockade with Milatuzumab or PI3K inhibition with LY294002 (**Figure 10A-C**). Flow cytometric analysis of CD206 expression yielded similar results (**Figure 10D**, **10E**).

To evaluate the involvement of downstream signaling pathways, the expression levels of PI3K, p-PI3K, AKT and p-AKT were analyzed. MCF7-derived CM increased the expression of p-PI3K and p-AKT compared with the control group, and these changes were attenuated following treatment with Milatuzumab or LY294002 (**Figure 10F**). Moreover, hypoxia-conditioned MCF7-derived CM increased the secretion of IL-10 and TGF-β1 by M2 macrophages, while these effects were attenuated following CD74 blockade or PI3K inhibition (**Figure 10G**, **10H**). These findings demonstrate that hypoxia-induced MIF promotes macrophage M2 polarization through CD74-mediated activation of the PI3K-AKT signaling pathway.

## Discussion

BRCA is a life-threatening malignancy with a high incidence among female cancers [1]. The present study revealed a critical mechanistic link between hypoxia-induced MIF secretion from BRCA cells and macrophage polarization, providing new insights into TME remodeling and potential therapeutic strategies. Hypoxia acts as an important driver of MIF upregulation in cancer cells, which in turn contributes to immune evasion and the establishment of pro-tumorigenic macrophage phenotypes. MIF is a cytokine secreted by tumor cells and functions as a ligand for CD74, a cell membrane-associated receptor. Upon binding to CD74, MIF activates downstream signaling cascade, leading to the release of CD74 cytosolic intracellular domain, which regulates transcriptional responses in immune cells [23].

CD74 plays an important role in BRCA progression. CD74 promotes tumor growth by inducing the expansion of tumor-infiltrating regulatory B cells and tolerogenic dendritic cells in TNBC [23]. Shi et al. reported that CD74 expression was elevated in tumor tissues across multiple cancer types compared with corresponding normal tissues [24]. Consistent with these findings, our results demonstrated that CD74 was significantly upregulated in BRCA tissues and predominantly expressed in macrophages within the tumor microenvironment, and that CD74 expression was associated with patient prognosis. Tian et al. reported that CD74 was positively expressed in 80.69% of BRCA cases and was significantly associated with lymph node metastasis and TNBC [25]. Previous studies have shown that CD74 promotes the proliferation, invasion, and migration of BRCA cells [26, 27]. Greenwood et al. reported that Stat1/CD74-positive TNBC exhibited more aggressive biological characteristics [28]. Wang et al. demonstrated that CD74 mRNA and protein levels were significantly increased in TNBC and were closely associated with cancer stem cell properties and epithelial-mesenchymal transition characteristics [29]. Moreover, a multi-omics study revealed that CD74 expression was significantly upregulated in most cancers compared with matched normal tissues and exhibited prognostic and predictive value [30].

MIF plays a critical role in BRCA progression through the MIF-CD74 axis. In this study, we observed that MIF was predominantly expressed in mammary epithelial cells, with significantly higher expression levels in the epithelial cells of BRCA tissue than those in normal breast tissue. Based on these findings, we hypothesized that MIF secreted by BRCA cells binds to CD74 expressed on macrophage membranes, thereby modulating macrophage function and contributing to BRCA progression. Our results revealed that MIF secreted by MCF7 cells promoted M2 polarization and increased the secretion of IL-10 and TGF-β1 from macrophages through interaction with the surface receptor CD74 on macrophages. The binding of MIF to CD74 may activate downstream signaling pathways, including the MAPK or PI3K-AKT signaling pathways, thereby regulating macrophage survival, migration, polarization, and other functional responses. Consistent with these findings, our study showed that MCF7-derived MIF promoted M2 polarization by activating the PI3K-AKT signaling pathway. In brain tumors, tumor-derived MIF promoted microglial polarization toward an M2 phenotype by acti-

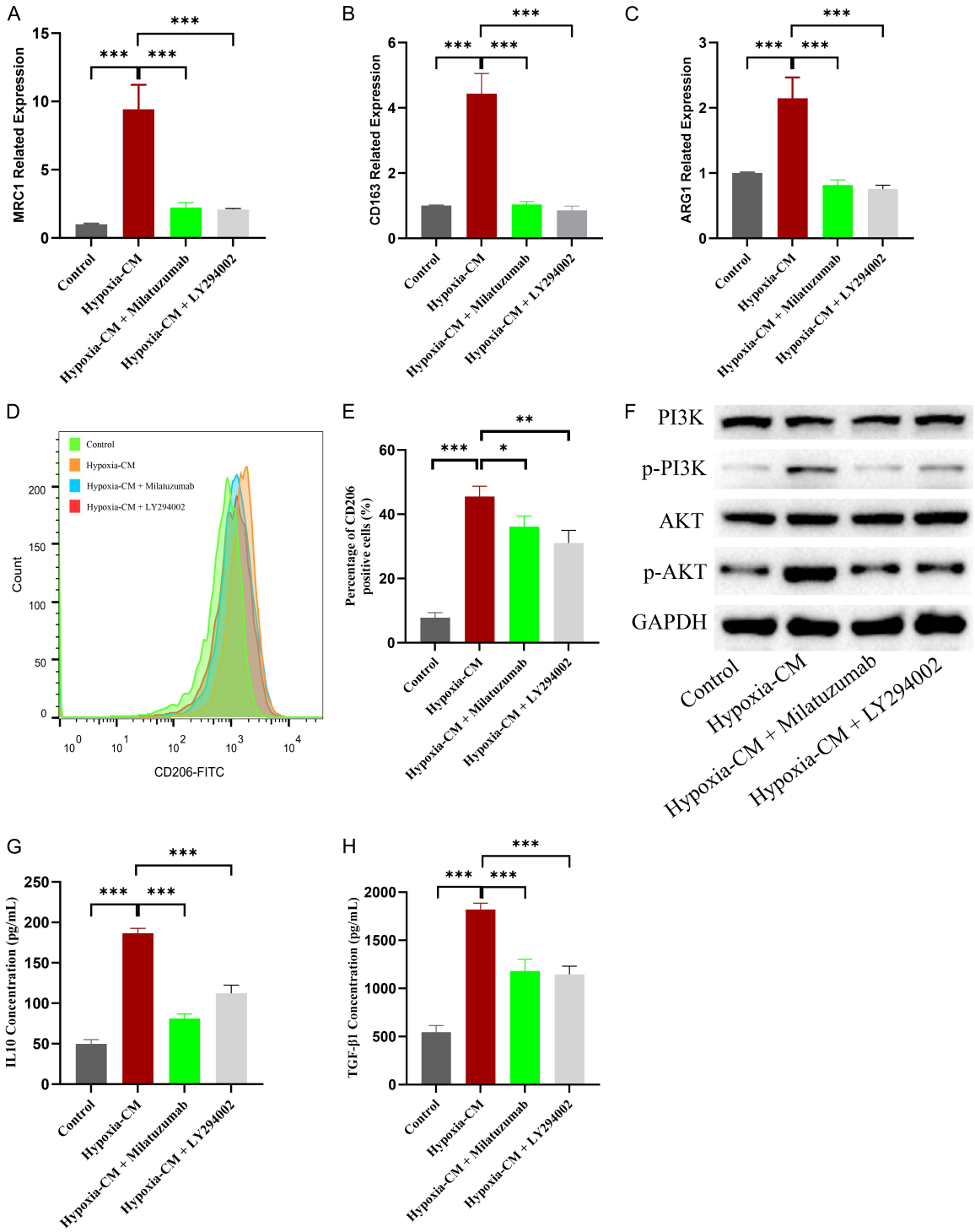



**Figure 10.** PI3K/AKT signaling is required for MIF/CD74-mediated macrophage M2 polarization. A. The mRNA expression of MRC1 (CD206). B. The mRNA expression of CD163. C. The mRNA expression of ARG1. D. Flow cytometry analysis of CD206 expression on macrophages. E. Percentage of CD206-positive macrophages. F. Western blot analysis of PI3K-AKT signaling pathway activation. G. Concentration of IL-10 in macrophage culture supernatants under different co-culture conditions. H. Concentration of TGF-β1 in macrophage culture supernatants under different co-culture conditions. Notes: *, $P < 0.05$; **, $P < 0.01$; ***, $P < 0.001$.

vating CD74 signaling, which inhibited interferon-γ secretion through phosphorylation of microglial ERK1/2 [31]. MIF also induced neutrophil accumulation in the alveolar space

through MIF's interaction with CD74 on alveolar macrophages, followed by activation of the p44/p42 MAPK pathway and subsequent release of neutrophil-recruiting chemokines [32]. Furthermore, MIF binding to the CD74-CD44 receptor complex on macrophage surfaces impaired amyloid-beta plaque clearance, thereby exacerbating Alzheimer's disease pathology [33]. Our intervention experiments using ISO-1 (MIF inhibitor) and Milatuzumab (anti-CD74) extended these findings by demonstrating that MCF7-derived MIF preferentially promoted M2-like polarization, consistent with the anti-apoptotic and pro-angiogenic functions of M2 macrophages in hypoxic TMEs [7, 34].

Hypoxia is a common characteristic of solid tumors. MIF is an essential regulator involved in tumorigenesis, angiogenesis, and tumor metastasis. Previous studies have demonstrated that MIF expression is elevated in Hep2 cells under hypoxic conditions [35]. Consistently, our study showed that MCF7 cells produced significantly higher levels of MIF under hypoxic conditions than under normoxic conditions. MIF contributes to tumor adaptation to hypoxic stress by promoting HIF-1α stabilization. Hahne et al. reported that MIF was redundantly regulated by HIF-1 and HIF-2 pathways [36]. Liu et al. reported that MIF was highly expressed in non-small cell lung cancer and was associated with prognosis [13]. Under hypoxic conditions, HIF-1α protein stability is enhanced, resulting in its intracellular accumulation. As a transcription factor, HIF-1α binds to the MIF promoter and promotes MIF transcription. Zhu et al. reported that MIF expression was reduced following knockdown of HIF-1α and HIF-2α in head and neck squamous cell carcinoma cells [37]. Therefore, targeting MIF using small-molecule antagonists may represent a potential therapeutic strategy for hypoxia-driven tumors.

It is important to acknowledge that the in vitro functional experiments in this study were conducted exclusively using the MCF7 cell line, which represents the luminal A ($ER^+$) subtype of breast cancer. In contrast, our transcriptomic analyses incorporated datasets covering multiple molecular subtypes. Given that breast cancer is characterized by substantial inter- and intra-tumoral heterogeneity, the use of a single cell line may limit the generalizability of our findings. Therefore, the conclusions derived from cellular experiments should be interpreted with caution. Further validations using additional breast cancer models, including $HER2^+$, and TNBC cell lines, are warranted to confirm whether the observed effects are subtype-specific or universally applicable across different biological contexts.

## Conclusions

This study identified a novel mechanism by which the MIF-CD74 axis promoted BRCA progression through regulation of macrophage M2 polarization and highlighted the crucial role of hypoxia in this process. Targeting the MIF-CD74 interaction may represent a potential therapeutic strategy for BRCA treatment.

## Acknowledgements

This work was supported by the National Natural Science Foundation of China (No. 822-60867).

## Disclosure of conflict of interest

None.

**Address correspondence to:** Jing Leng, Department of Immunology, School of Basic Medical Sciences, Guangxi Medical University, No. 22 Shuangyong Road, Nanning 530021, Guangxi, China. E-mail: lj986771558@163.com; Shengkang Dai, Department of Gynecology, The Second Affiliated Hospital of Guangxi University of Chinese Medicine, No. 10 Huadong Road, Nanning 530011, Guangxi, China. E-mail: daishengkang111@163.com

## References

[1] Siegel RL, Kratzer TB, Giaquinto AN, Sung H and Jemal A. Cancer statistics, 2025. CA Cancer J Clin 2025; 75: 10-45.

[2] Wowui PI, Mprah R, Ndzie Noah ML, Adu-Amankwaah J, Kanoseh AWL, Tao L, Chulu D, Yalley SK, Shaheen S and Sun H. Estrogen via GPER downregulated HIF-1a and MIF expression, attenuated cardiac arrhythmias, and myocardial inflammation during hypobaric hypoxia. Mol Med 2025; 31: 107.

[3] Jeong H, Lee SY, Seo H and Kim BJ. Recombinant *Mycobacterium smegmatis* delivering a fusion protein of human macrophage migration inhibitory factor (MIF) and IL-7 exerts an anticancer effect by inducing an immune response against MIF in a tumor-bearing mouse

model. J Immunother Cancer 2021; 9: e003180.
[4] Youness RA, Elemam NM, Abdelhamid AM, Mohamed AH, Elsherbiny LM, Ramzy A and Assal RA. Macrophage migration inhibitory factor (MIF) and the tumor ecosystem: a tale of inflammation, immune escape, and tumor growth. Front Immunol 2025; 16: 1636839.
[5] You B, Zhang J, Yang C, Dun Y, Qi D, Long Y, Cheng J, Lin Y, Zhou N, Zeng T, Dong J and Liu S. Salidroside protects against myocardial infarction via activating MIF-mediated mitochondrial quality control. Chin Med 2025; 20: 27.
[6] Semenza GL. Mechanisms of breast cancer stem cell specification and self-renewal mediated by hypoxia-inducible factor 1. Stem Cells Transl Med 2023; 12: 783-790.
[7] Zhi S, Chen C, Huang H, Zhang Z, Zeng F and Zhang S. Hypoxia-inducible factor in breast cancer: role and target for breast cancer treatment. Front Immunol 2024; 15: 1370800.
[8] Verjans E, Noetzel E, Bektas N, Schütz AK, Lue H, Lennartz B, Hartmann A, Dahl E and Bernhagen J. Dual role of macrophage migration inhibitory factor (MIF) in human breast cancer. BMC Cancer 2009; 9: 230.
[9] Yan L, Wu M, Wang T, Yuan H, Zhang X, Zhang H, Li T, Pandey V, Han X, Lobie PE and Zhu T. Breast cancer stem cells secrete MIF to mediate tumor metabolic reprogramming that drives immune evasion. Cancer Res 2024; 84: 1270-1285.
[10] Lue H, Thiele M, Franz J, Dahl E, Speckgens S, Leng L, Fingerle-Rowson G, Bucala R, Lüscher B and Bernhagen J. Macrophage migration inhibitory factor (MIF) promotes cell survival by activation of the Akt pathway and role for CSN5/JAB1 in the control of autocrine MIF activity. Oncogene 2007; 26: 5046-5059.
[11] Wirtz TH, Saal A, Bergmann I, Fischer P, Heinrichs D, Brandt EF, Koenen MT, Djudjaj S, Schneider KM, Boor P, Bucala R, Weiskirchen R, Bernhagen J, Trautwein C and Berres ML. Macrophage migration inhibitory factor exerts pro-proliferative and anti-apoptotic effects via CD74 in murine hepatocellular carcinoma. Br J Pharmacol 2021; 178: 4452-4467.
[12] Yang H, Li J, Huang XR, Bucala R, Xu A and Lan HY. Macrophage-derived macrophage migration inhibitory factor mediates renal injury in anti-glomerular basement membrane glomerulonephritis. Front Immunol 2024; 15: 1361343.
[13] Liu L, Wang J, Wang Y, Chen L, Peng L, Bin Y, Ding P, Zhang R, Tong F and Dong X. Blocking the MIF-CD74 axis augments radiotherapy efficacy for brain metastasis in NSCLC via synergistically promoting microglia M1 polarization. J Exp Clin Cancer Res 2024; 43: 128.
[14] Quail DF and Joyce JA. Microenvironmental regulation of tumor progression and metastasis. Nat Med 2013; 19: 1423-1437.
[15] Laoui D, Movahedi K, Van Overmeire E, Van den Bossche J, Schouppe E, Mommer C, Nikolaou A, Morias Y, De Baetselier P and Van Ginderachter JA. Tumor-associated macrophages in breast cancer: distinct subsets, distinct functions. Int J Dev Biol 2011; 55: 861-867.
[16] Leek RD, Lewis CE, Whitehouse R, Greenall M, Clarke J and Harris AL. Association of macrophage infiltration with angiogenesis and prognosis in invasive breast carcinoma. Cancer Res 1996; 56: 4625-4629.
[17] Mantovani A, Sozzani S, Locati M, Allavena P and Sica A. Macrophage polarization: tumor-associated macrophages as a paradigm for polarized M2 mononuclear phagocytes. Trends Immunol 2002; 23: 549-555.
[18] Ojalvo LS, King W, Cox D and Pollard JW. High-density gene expression analysis of tumor-associated macrophages from mouse mammary tumors. Am J Pathol 2009; 174: 1048-1064.
[19] Ojalvo LS, Whittaker CA, Condeelis JS and Pollard JW. Gene expression analysis of macrophages that facilitate tumor invasion supports a role for Wnt-signaling in mediating their activity in primary mammary tumors. J Immunol 2010; 184: 702-712.
[20] Pucci F, Venneri MA, Biziato D, Nonis A, Moi D, Sica A, Di Serio C, Naldini L and De Palma M. A distinguishing gene signature shared by tumor-infiltrating Tie2-expressing monocytes, blood "resident" monocytes, and embryonic macrophages suggests common functions and developmental relationships. Blood 2009; 114: 901-914.
[21] Uhlén M, Fagerberg L, Hallström BM, Lindskog C, Oksvold P, Mardinoglu A, Sivertsson Å, Kampf C, Sjöstedt E, Asplund A, Olsson I, Edlund K, Lundberg E, Navani S, Szigyarto CA, Odeberg J, Djureinovic D, Takanen JO, Hober S, Alm T, Edqvist PH, Berling H, Tegel H, Mulder J, Rockberg J, Nilsson P, Schwenk JM, Hamsten M, von Feilitzen K, Forsberg M, Persson L, Johansson F, Zwahlen M, von Heijne G, Nielsen J and Pontén F. Proteomics. Tissue-based map of the human proteome. Science 2015; 347: 1260419.
[22] Li C, Tang Z, Zhang W, Ye Z and Liu F. GEPIA2021: integrating multiple deconvolution-based analysis into GEPIA. Nucleic Acids Res 2021; 49: W242-W246.
[23] Pellegrino B, David K, Rabani S, Lampert B, Tran T, Doherty E, Piecychna M, Meza-Romero R, Leng L, Hershkovitz D, Vandenbark AA, Bucala R, Becker-Herman S and Shachar I. CD74 promotes the formation of an immunosuppressive tumor microenvironment in triple-

negative breast cancer in mice by inducing the expansion of tolerogenic dendritic cells and regulatory B cells. PLoS Biol 2024; 22: e3002905.
[24] Shi WQ, Chen DX, Du ZS, Liu CP, Zhai TT, Pan F, Chen HL, Liao WN, Wang SH, Fu JH, Qiu SQ and Wu ZY. CD74 is a potential biomarker predicting the response to immune checkpoint blockade. Cancer Cell Int 2024; 24: 340.
[25] Tian B, Zhang Y, Li N, Liu X and Dong J. CD74: a potential novel target for triple-negative breast cancer. Tumour Biol 2012; 33: 2273-2277.
[26] Ssadh HA, Abdulmonem WA, Rasheed Z, Madar IH, Alhoderi J, Eldeen SKN, Alradhwan A, Alasmael N, Alkhamiss A and Fernández N. Knockdown of CD-74 in the proliferative and apoptotic activity of breast cancer cells. Open Access Maced J Med Sci 2019; 7: 3169-3176.
[27] Liu Z, Chu S, Yao S, Li Y, Fan S, Sun X, Su L and Liu X. CD74 interacts with CD44 and enhances tumorigenesis and metastasis via RHOA-mediated cofilin phosphorylation in human breast cancer cells. Oncotarget 2016; 7: 68303-68313.
[28] Greenwood C, Metodieva G, Al-Janabi K, Lausen B, Alldridge L, Leng L, Bucala R, Fernandez N and Metodiev MV. Stat1 and CD74 overexpression is co-dependent and linked to increased invasion and lymph node metastasis in triple-negative breast cancer. J Proteomics 2012; 75: 3031-3040.
[29] Wang J, Huang D, Nguyen TAT, Phan LM, Wei W and Rezaeian AH. CD74-AKT axis is a potential therapeutic target in triple-negative breast cancer. Biology (Basel) 2024; 13: 481.
[30] Li RQ, Yan L, Zhang L, Zhao Y and Lian J. CD74 as a prognostic and M1 macrophage infiltration marker in a comprehensive pan-cancer analysis. Sci Rep 2024; 14: 8125.
[31] Ghoochani A, Schwarz MA, Yakubov E, Engelhorn T, Doerfler A, Buchfelder M, Bucala R, Savaskan NE and Eyüpoglu IY. MIF-CD74 signaling impedes microglial M1 polarization and facilitates brain tumorigenesis. Oncogene 2016; 35: 6246-6261.
[32] Takahashi K, Koga K, Linge HM, Zhang Y, Lin X, Metz CN, Al-Abed Y, Ojamaa K and Miller EJ. Macrophage CD74 contributes to MIF-induced pulmonary inflammation. Respir Res 2009; 10: 33.
[33] Liu B, Luo W, Huang L, Wei C, Huang X, Liu J, Tao R, Mo Y and Li X. Migration inhibition factor secreted by peripheral blood memory B cells binding to CD74-CD44 receptor complex drives macrophage behavior in Alzheimer's disease. Am J Alzheimers Dis Other Demen 2024; 39: 15333175241238577.
[34] Vámos E, Vántus VB, Deák P, Kálmán N, Sturm EM, Nayak BB, Makszin L, Loránd T, Gallyas FJ and Radnai B. MIF tautomerase inhibitor TE-11 prevents inflammatory macrophage activation and glycolytic reprogramming while reducing leukocyte migration and improving Crohn's disease-like colitis in male mice. Front Immunol 2025; 16: 1558079.
[35] Yang M, Wu S, Cai W, Ming X, Zhou Y and Chen X. Hypoxia-induced MIF induces dysregulation of lipid metabolism in Hep2 laryngocarcinoma through the IL-6/JAK-STAT pathway. Lipids Health Dis 2022; 21: 82.
[36] Hahne M, Schumann P, Mursell M, Strehl C, Hoff P, Buttgereit F and Gaber T. Unraveling the role of hypoxia-inducible factor (HIF)-1α and HIF-2α in the adaption process of human microvascular endothelial cells (HMEC-1) to hypoxia: Redundant HIF-dependent regulation of macrophage migration inhibitory factor. Microvasc Res 2018; 116: 34-44.
[37] Zhu G, Tang Y, Geng N, Zheng M, Jiang J, Li L, Li K, Lei Z, Chen W, Fan Y, Ma X, Li L, Wang X and Liang X. HIF-α/MIF and NF-κB/IL-6 axes contribute to the recruitment of CD11b+Gr-1+ myeloid cells in hypoxic microenvironment of HNSCC. Neoplasia 2014; 16: 168-179.